HAL
open science

Flow Spectral Analysis in a Wake of a Self-Sustained Oscillating Airfoil

Azemi Benaissa

Flow Spectral Analysisin the Wake of a Self-Sustained Oscillating Airfoil

L. Goyaniuk[a], C. ItwarBarrett[b], D. Poirel[c] and A. Benaissa[d,*]

Royal Military College of Canada, Kingston, Ontario K7K 7B4
[a]Luba.Goyaniuk@rmc.ca, [b]Crystal.Itwar-Barrett@rmc.ca, [c]Poirel-d@rmc.ca,
[d,*]benaissa-a@rmc.ca

Résumé:

Dans cette étude, le champ de vitesse dans le sillage à l'arrière d'une aile rigide montée sur un support flexible est analysé. L'objet principal était la structure du sillage généré derrière l'aile durant ses mouvements en tangage et battement , résultants de l'interaction mutuelle entre l'écoulement et l'aile. L'aile utilisée est de profil NACA0012, l'axe élastique est situé à 35% de la corde à partir du bord d'attaque. L'étude a été menée pour différents nombres de Reynolds dans la gamme 7.5 x 10^4 ≤ Re$_c$ ≤ 1.3 x 10^5, où des oscillations entretenues de larges amplitudes en xxxx et yyyy sont observées. L'anémométrie à fils chauds a été utilisée pour mesurer la fluctuation de la composante de vitesse dans le sens de l'écoulement. Il en résulte l'apparition dans les spectres de vitesse d'un pic à la fréquence double de la fréquence d'oscillation de l'aile. L'analyse a aussi montré l'absence de l'allée de Kármán dans le sillage ainsi qu'une distribution des échelles dans l'écoulement qui suit l'allure d'une zone inertielle avec une puissance en -5/3 sur presque deux décades.

Abstract:

In this study, the velocity field in the wake behind a rigid airfoil mounted on a flexiblesupport is analyzed. The main focuswason the wake structures generated in the flow behind the airfoil during the pitchingand heavingmotions of the airfoil, resulting from the feedback interaction of the flow and the structure. The airfoil used is a NACA0012;the elastic axis was located at 35% of the chord length from the leading edge. The study was carried out at different Reynolds numbers in the range of 7.5 x 10^4 ≤ Re$_c$ ≤ 1.3 x 10^5, where large amplitude self-sustained oscillating motions in pitch and heave are observed. Hot wire anemometry was used to record velocity fluctuations along the main flow direction. It resulted in the appearance on the velocity spectra of a dominant peak at twice the frequency of airfoil oscillation. The analysis also showed an absenceof Kármán vortices in the wake and that the scale distribution in thisflow follows very well an inertial subrange behavior with a -5/3 power law over almost two decades.

Key words: Experiment / Fluid-Structure Interaction / Self-Sustained Oscillations / Low Reynolds number Aerodynamics/Wind Energy Extraction.

NOMENCLATURE:

A	projected area of the airfoil
C	airfoil cord length
D_θ	structural damping coefficient
$E(f)$	Power spectrum
f	frequency (Hz)
I_{EA}	moment of inertia about the elastic axis
k	reduced frequency
K_θ	stiffness in pitch
K_h	stiffness in heave
M_{EA}	moment in pitch
M_h	mass in translation
P	power extracted
P_a	power available in the flow
Rec	Reynolds Number
St	Strouhal Number
u, v	axial and transversal velocity fluctuation

u'	RMS value of u
U	axial mean velocity

Acronyms

DOF	degree of freedom
LCO	limit-cycle oscillation
LEV	leading edge vortex
LSB	laminar separation bubble
UAV	unmanned aerial vehicle

Greek symbols

η	Efficiency
ω	Frequency in rd/s
$\overline{\theta^2}$	variance of the pitch amplitude

Subscript

EA	elastic axis
C	cord length
θ	pitch
h	heave
∞	Free stream

Introduction

With the advent of rapid development of unmanned air vehicles (UAVs), the characterization of the unsteady flow phenomenon, as well as the accompanying aerodynamic loads has been the subject of recent research. The operational range of some UAVs falls within the 'moderate' Reynolds number range, between $10^4 \leq \text{Re}_c \leq 10^6$. Within this regime, complex viscous phenomena occur; they have a significant impact on elastic airfoil behaviour, and the subsequent aeroelastic response. The unsteady viscous flow can be separating or reattaching over a large portion of the top surface of the airfoil. The predominant feature of dynamic stall for example, is the formation, shedding and convection over the upper surface of the airfoil of an energetic vortex-like disturbance. This convection induces a fluctuating pressure field, and produces transient variations in forces and moments that are fundamentally different from steady-state aerodynamics. Investigations on the convection of the leading-edge vortex (LEV) due to prescribed oscillations have been studied in the context of biological flight, highly manoeuvrable UAVs, and much more recently, passive energy extraction applications.

In a fairly recent study performed by Lee and Gerontakos[1], hot-film measurements, supplemented with hot-wire measurements and smoke-flow visualizations, were undertaken to characterize the boundary layer and wake of a NACA 0012 airfoil at a Reynolds number of 1.35×10^5. They considered the static, andthe cases were the airfoil was pitching at small and large pitch amplitudes.A wake vortex pattern was found to exist, which was similar in characteristics to a von Kármán type of shedding. A laminar separation bubble was also present. Unlike the static case, the LSB size decreases and moves toward the leading edge when the incidence angle continues to increase. The characteristics of the unsteady boundary layer for the large angle oscillations were seen to be much more complicated compared to the small angle oscillations. The subsequent growth and convection of an energetic LEV was observed as the airfoil continued to pitch up past the static-stall angle, at 21.9°. This includes the onset and end of the upward spreading of flow reversal, characterized by narrower turbulent fields, followed by a breakdown of the turbulent boundary layer and convection of the LEV. The results from the study disproved a previously held notion that leading-edge dynamic stall originates with the bursting of a laminar separation bubble.

There are few experiments in related literature that have focused on characterizing the flow about a wing undergoing limit-cycle oscillations due to nonlinear aeroelastic phenomena within transitional Reynolds numbers. Previous related investigations focused on the small amplitude LCO's occurring as a result of the influence of a LSB. Initial measurements by Benaissa and Poirel [2] of the longitudinal (*u*) and normal (*v*) velocity components were done on an elastically mounted rigid wing with a NACA 0012 profile of constant chord. The spectra of both the *u* and *v* components show the oscillation frequency of the airfoil, as well as the shedding frequency of the static airfoil. It was determined to be a clear consequence of the low frequency vortex associated with the oscillation on the Kármán type vortex shedding. Further experiments by Rudminet al.[3] using hot-film sensor responses on a motor driven wing, confirmed the behavior of the LSB within a range of moderate Reynolds numbers, for the NACA 0012 set-up discussed. As determined by Lee and Gerontakos[1], the size of the separation bubble is reduced and travels towards the leading-edge when the angle of attack increases, and when the Reynolds number increases. Poels et al [4] further confirmed use of the motor-driven pitching wing with hot-film sensor signals to characterize the behaviour of the LSB. The *u* and *v* velocity components were recorded in the wake of the motor driven oscillating airfoil with a cross hot wire probe. The spectra of the wake were determined for a wide range of Reynolds numbers, and it was observed that the free airfoil has a more pronounced vortex shedding peak. Conversely, a more pronounced peak was found to form for the motor driven airfoil at higher Strouhal numbers for higher Reynolds numbers.

Numerical simulations by Yuan *et al.*[5] were performed for one-degree-of freedom and two-degree-of freedom heave small amplitude LCO's. Three dimensional large-eddy-simulation (LES) results confirmed the presence of these oscillations for the aforementioned set-up, at a Reynolds number of 7.7×10^4. The amplitude of oscillation and frequency, as well as the work done by the aerodynamic moment obtained from numerically were found to be in excellent agreement with previous experimental results. It was also observed that, due to the delayed recovery of the flowfield when compared to the corresponding static conditions at the respective

angle of attack, the separation and turbulent reattachment of the LSB caused negative aerodynamic damping. The resulting negative aerodynamic damping fed energy to the aeroelastic LCO's when coupled with the freely oscillating airfoil. Plotting the aerodynamic pitching-moment coefficient as a function of the pitch angle revealed an overall clockwise loop during one 1DOF LCO cycle, thus indicating a positive work done by the flow near the static equilibrium position. The loop of the lift coefficient as a function of the heave displacement was also clockwise, indicating a positive work done by the lift force as well.

While 1DOF small amplitude LCO's occur due to the negative aerodynamic damping caused by a feedback coupling mechanism between the LSB behavior and the structural response, 1DOF large amplitude LCO's can occur as a result of stall flutter. Stall flutter is an aeroelastic dynamic phenomenon associated with dynamic stall as a wing pitches in and out of leading-edge separation conditions at large pitch amplitudes, thus inducing negative aerodynamic damping for part of the cycle. It is fundamentally a non-linear problem in 1DOF pitching motion, and is triggered by a large amplitude disturbance if the wing is initially resting at small angle of attack equilibrium. When instability is induced, the oscillation grows until it reaches a non-linear dynamic stable state. While investigations have focussed on investigating LSB characteristics about passive aeroelastic responses, there remains much to be understood about the unsteady flow associated with stall flutter.

In a recent study by Onoue and Breuer [6], particle-image velocimetry (PIV) measurements were carried out in order to investigate the flow structure about a passively pitching plate undergoing 1DOF stall flutter LCO's about the mid-chord, at a Reynolds number of 9.9×10^4. Measurements of the wake were performed to characterize the behaviour of the separated flow structures and their relation to the plate kinematics and unsteady aerodynamic torque generation. The visualizations and torque measurements exhibited the classic features of dynamic stall, where the aerodynamic force and torque on the plate are significantly augmented by the formation and growth of a strong LEV on the suction side of the plate. The LEV core was observed to grow in strength and size, as it entrained circulation of the small eddies at the leading edge. An interesting observation was the train of opposite-signed vortices continuously shed from the trailing-edge. In addition, it was noted that the shedding frequency associated with the smaller eddies was much higher than that of the primary vortices, which was comparable with the pitching frequency. As the LEV was convected towards the trailing-edge, the plate experienced a sharp drop in the aerodynamic torque while continuing to rotate towards a maximum angle of 90°. Interestingly, upon reaching the maximum angle of rotation, a second increase in the aerodynamic torque was observed due to the development of a secondary vortex at the leading-edge.

It is clear that within thetransitional range of Reynolds numbers, the flow structure has a significant impact on elastic airfoil behavior, and on the subsequent aeroelastic response. In this study, the wake vortex shedding is analyzed for large amplitude pitch and heave LCO's due to stall flutter. The objective of this study is to understand the aeroelastic feedback effect of the structure on the flow by characterizing its signature in the wake.

Experimental setup

The experiment was carried out in a closed loop wind tunnel shown in Figure 1. The contraction factor of the convergent is 1:11.5 and the test section is 76cm x 108 cm. The level of turbulence intensity does not exceed 0.2 % for Reynolds Numbers below 130,000 used in this experiment. The apparatus is a two-degree-of-freedom system, composed of a rigid wing moving in translation (heave) and in rotation (pitch) as shown in Figure 2. Theairfoil is a NACA 0012 of constant chord length. The wingspan of the wing is 0.61 m, while thechord length is 0.156 m. The location of the elasticaxis is at 35% of the chord length from the leadingedge. The stiffness in pitch K_θ, was kept at a constantvalue of 0.3 N·m/rad. The structural damping wasassumed constant, and calculated by obtaining thedamping ratio from the logarithmic decrement of thenoflow free-decay response.

The value for thestructural damping coefficient D_θ, was calculated to be0.0011 N·m·s/rad. The frequency ratio,$\overline{\omega}$ defined below, was found to be 0.64.

$$\overline{\omega} = \frac{\omega_\theta}{\omega_h}$$
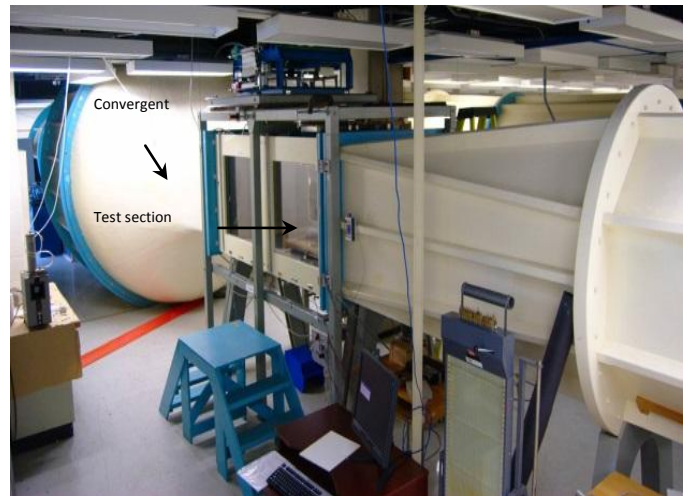

Figure 1: Wind tunnel used for the experiment.

Where, ω_θ and ω_h are defined as:

$$\omega_\theta = \sqrt{\frac{K_\theta}{I_{EA}}} \quad \text{and} \quad \omega_h = \sqrt{\frac{K_h}{M_h}}$$

The apparatus is capable of exhibiting fundamental wing aeroelastic phenomena, both linear and nonlinear, such as flutter, limit cycle oscillations andresponse to external turbulence.

In order to measure both the airfoil motion and the velocity simultaneously, 2 potentiometers and a hotwire probe were used.The probe was mounted to measure the longitudinal (u) component of the velocity in the wake of the airfoil at one cord length behind the airfoil. Velocity was measured using a DISA CTA bridge 56C17. The velocity fluctuations and pitch(or pitch and heave) signals were conditionedusing a WBK18 and an 8 channel dynamicsignal conditioningmodule anddigitized with a 16 bit AD Wavebook from IOTEC with a sampling frequency of 5 kHz. The schematic of the experiment setup and data acquisition is shown in Figure 3.
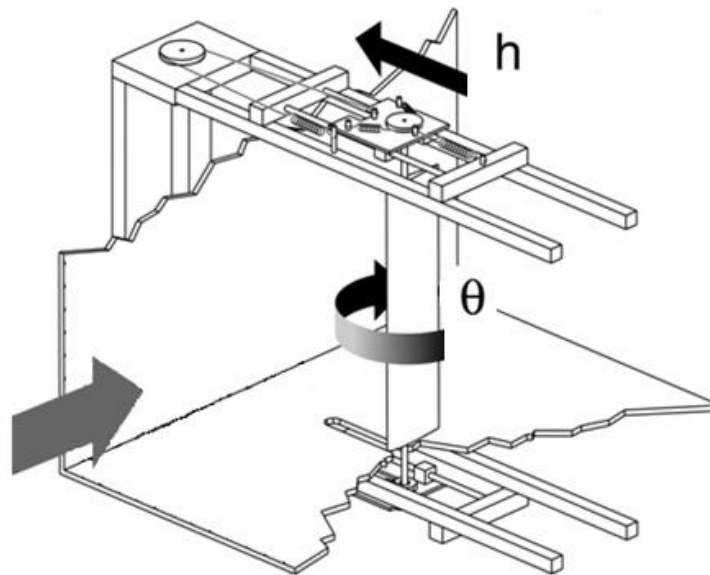

Figure 2: Aeroelastic Rig, free in heave (h) and pitch (θ).
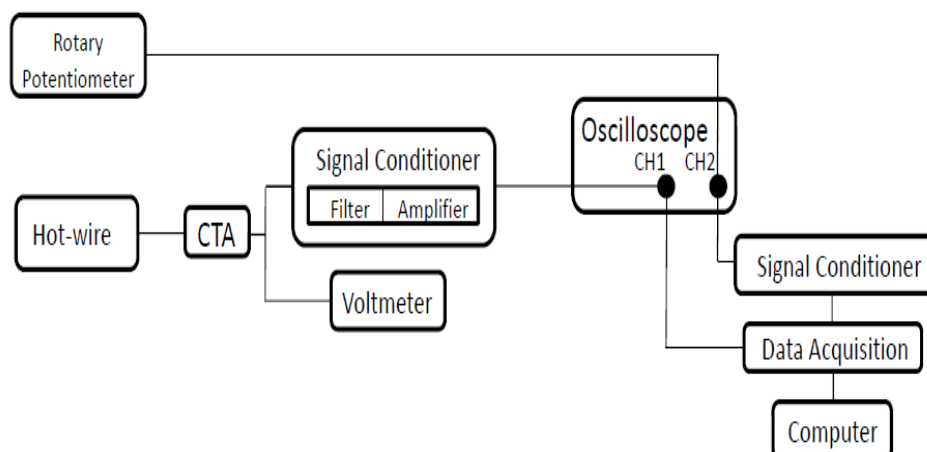
Figure 3: Schematic of the experimental set-up and data acquisition system

6

Results

   A spectral analysis, using an FFT algorithm, was performed on the velocity signals obtained in the wake of the static airfoil, one chord length behind the trailing edge and centred on the zero heave position. The peaks in the spectra presented in Figure4(shifted in amplitude for the a better presentation) indicate the shedding frequency behind the airfoil for a free stream velocity of 8.19 m/s and 12.56 m/s.These frequencies were determined to be 286.3Hz (St = 0.654), and 595.8 Hz (St = 0.888) ($\pm$ 0.15Hz) respectively.
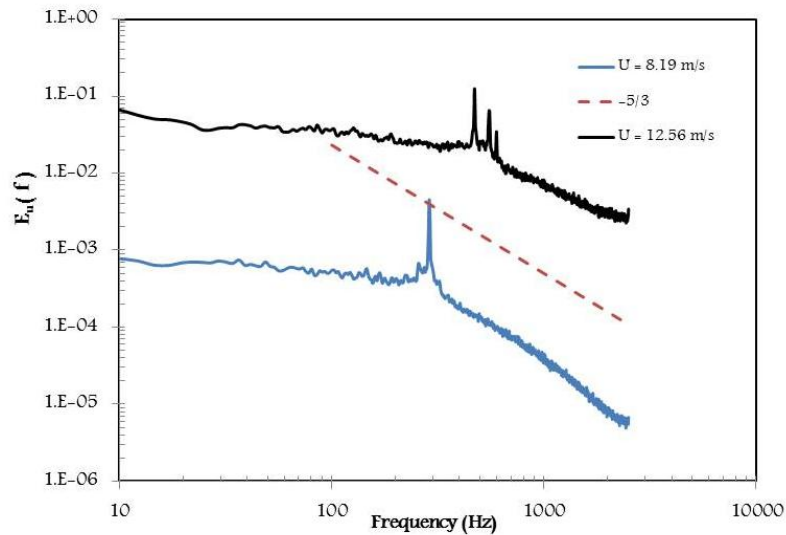

Figure 4: Spectra of the velocity fluctuations in the wake of the static airfoil.

   The signature of the Kármán vortex shed street is observed in the entire range of Reynolds numbers studied.The increase of Strouhal Number with Re_c agrees with the literature data (Huang and Lin [1998]).The dashed line plotted with the spectra represents the -5/3 slope, it indicates the inertial range. A small portion of the spectrum at U_∞ = 8.19 m/s, just after the peak frequency, shows the presence of a small inertial sub-range region. This region is not visible in the represented portion of the velocity spectrum at U_∞ = 12.56 m/s. This region is further away from the 3 peaksobserved at higher frequencies. The two small peaks are not harmonics of the fundamental peak at the higher airspeed.
   From the 2DOF data we represent the airfoil motion data in Figure 5. Both pitch and heave amplitudes increase with Re_c. The heave amplitude displays two tendencies (high rate of increase at the lower speeds and slower rate for higher speeds). The pitch amplitude seems to tend toward a plateau for higher Reynolds numbers.The reduced frequency defined as $k = \frac{\pi fc}{U_\infty}$ is multiplied by a 0.1 factor to be presented on the same scale range as the heave in meters, shown also in the same figure, decreases and tend to an asymptotic value that could be reached at higher speed than the ones tested in this experiment.
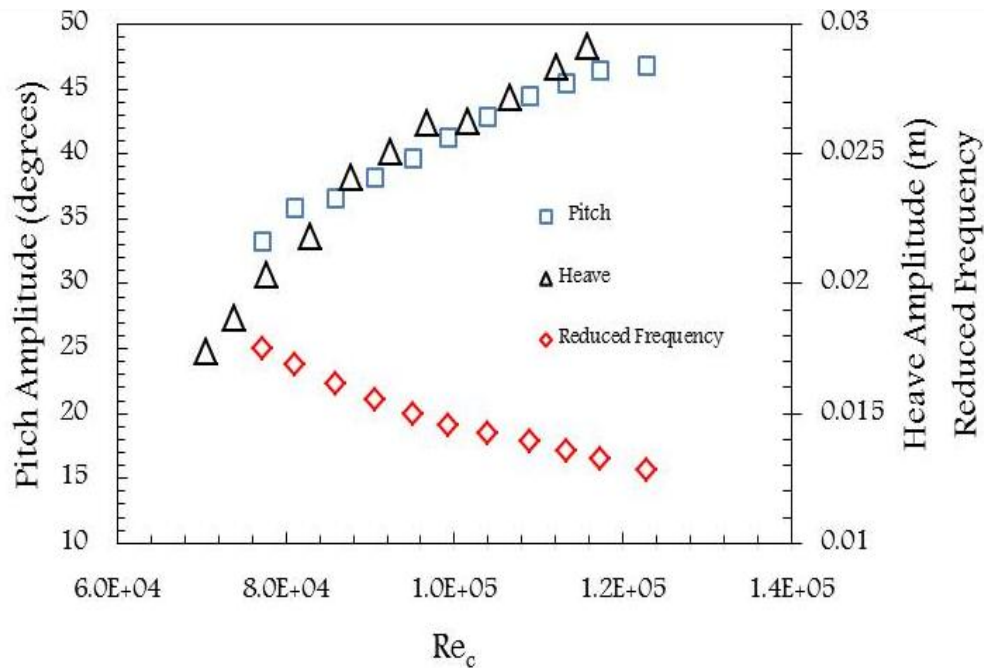
**Figure 5:** Pitch and Heave amplitude and reduced frequency for the 2 DOF LCO motion versus Re$_c$.

Its trend is similar to the pitch amplitude evolution.This frequency remains above a value of 0.05, indicating that unsteady effects are significant in the aerodynamics during LCO.

Samples of the pitch, heave and velocity signals as they vary with timeare presented in Figure 6. These sampleswere obtained at U$_\infty$ =10.6 m/s, they show the delay between the pitch and heave. This delay indicates that at the zero position in heave the airfoil has an incidence angle of about 0.5 of the maximum amplitude (~ 21°). It also shows that the velocity recorded is composed of intermittent turbulent spots centred on zero heave positions. These turbulent spots arrive on the measurement position with a time interval corresponding to half the period of the airfoil's oscillatory motion. They appear about three times during a pitching period. To better understand the effect of the airfoil motion on the wake,Spectral analysis was performed on the wake velocitybehind the wing undergoing 2DOF LCO.The pitch and heavedata obtained simultaneously with the velocity are also analysed, for a range of Reynolds numbers approximately 7.5 x 10^4 ≤ Re$_c$≤ 1.3 x 10^5 (7.5 m/s to 12 m/s). The corresponding spectral graphs for several airspeeds are included in Figure 7. The spectra are staggered for a better presentation. The pitch and heave spectra are represented for only U$_\infty$ = 8.34 m/s.
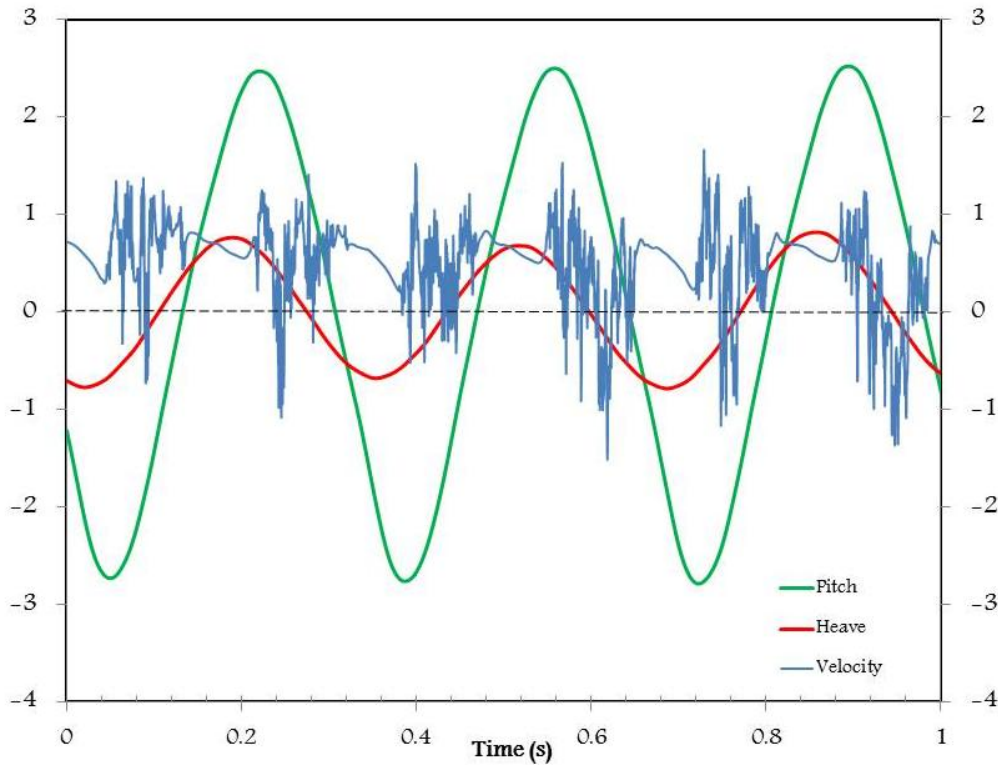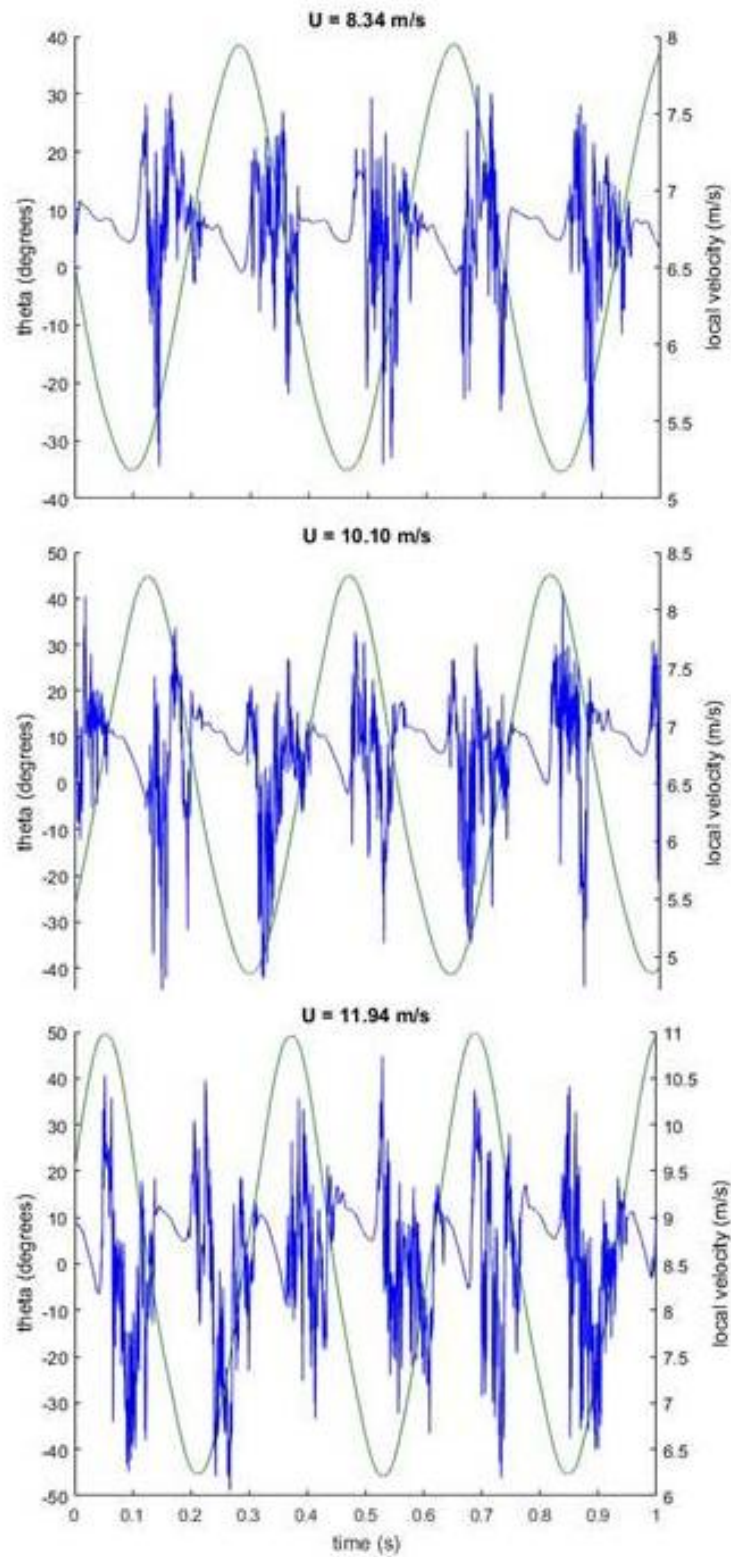
Figure 6: Pich, Heave and velocity variation with time for U_∞ = 10.6 m/s for the 2DOF LCO motion.

The dominant peaks in the velocity spectracorrespond to the first super harmonics of the airfoil oscillatory frequency. The signature of the oscillation frequency of the airfoil on the wake velocity is more pronounced for higher speeds than for the lower speeds. The dashed line crossing the spectra from low to high velocity represents the location of the Kármán vortex street obtained for fixed airfoil.It is determined that the Kármán vortices are not visible in the wake flow. The presence of these eddies were observed in previous studies for low amplitude oscillations Benaissa and Poirel [4] for the same range of velocities.
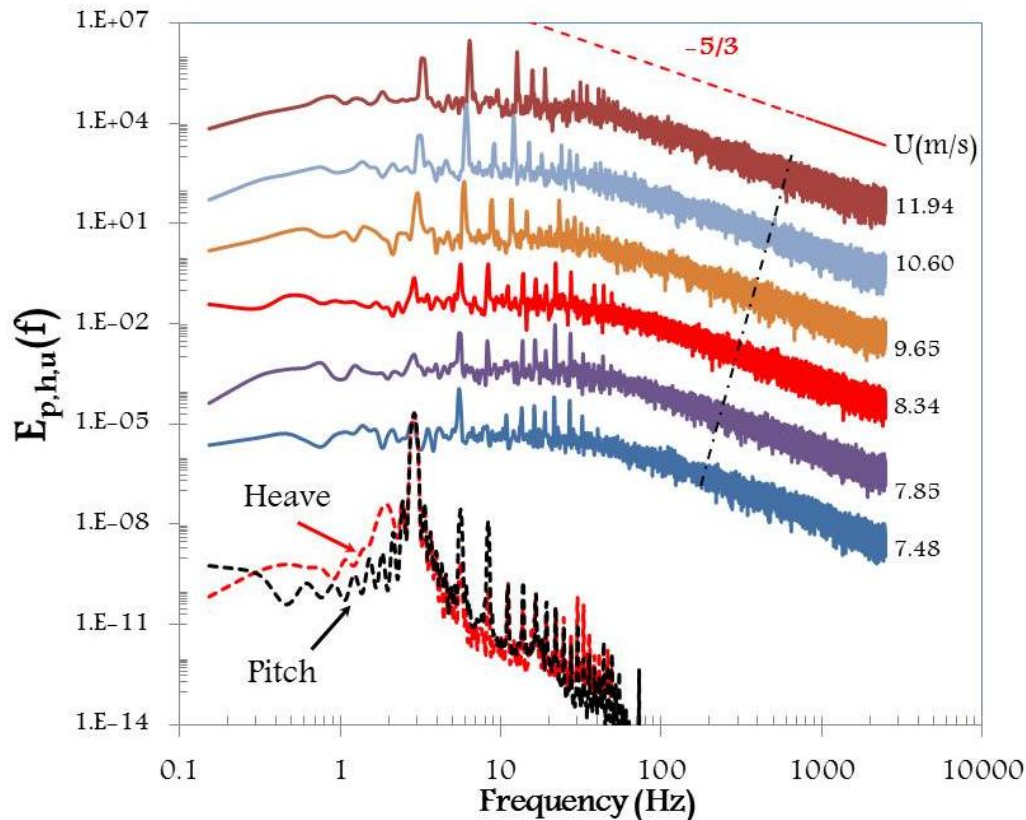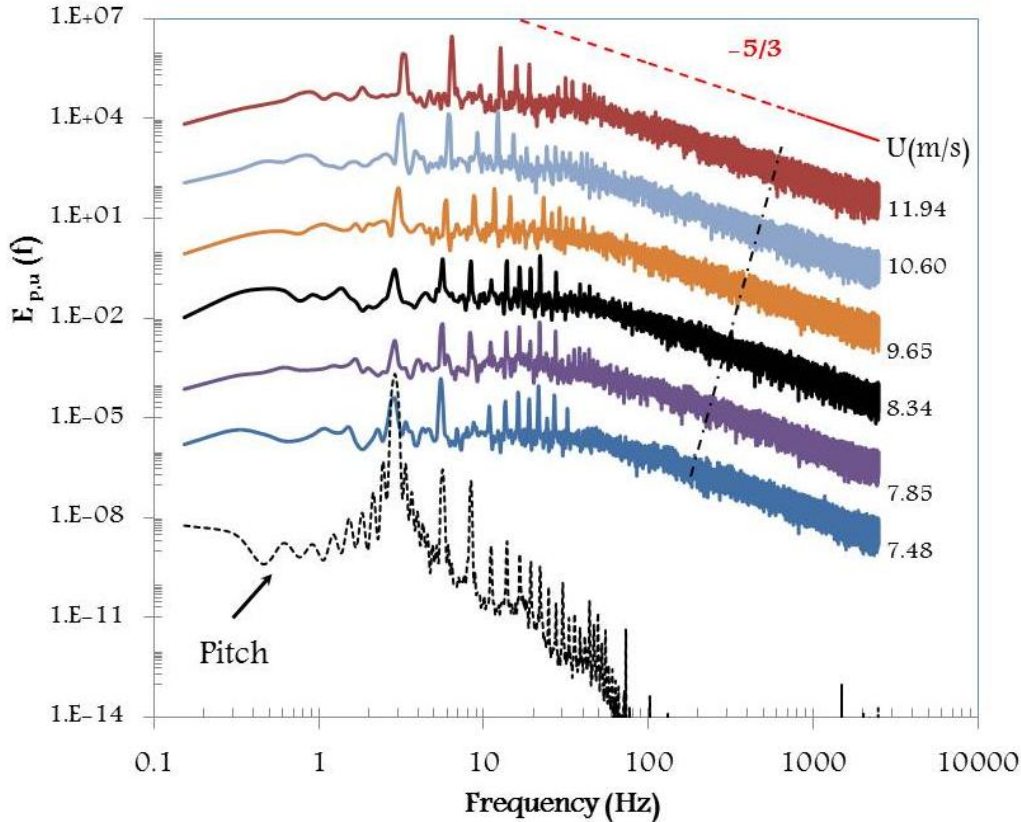
Figure 7: Pich, heave and velocity spectra of the 2DOF LCO motion.

The velocity spectra follow the -5/3 slope well after the attenuation of the harmonics (for almost two decades). This indicates that the motion of the airfoil produced a well-mixed wake where the inertial range is extended compared to the fixed airfoil (see Figure 3).To reduce the complexity of the flow in the wake, the airfoil was restrained to move only in pitch. For the same range of Reynolds where a 2DOF LCO was investigated, a 1DOF LCO was observed in pitch with high amplitude oscillation angles. With this new configuration, spectral analysis was also performed on the velocity data obtained in the wake of the wing undergoing 1DOF LCO in pitch.The wing behaves as a harmonic oscillator with a constant energy for a given speed. Contrary to the 2DOF case, the measurement position is more exposed to

Figure8: Pitch and velocity variation with time for different airspeeds for the 1DOF LCO motion.

thewake flow. The duration of the turbulent signals recorded is longer and the turbulence intensity is higher for the same speed than in the 2DOF case particularly at higher speeds (see Figure 8). As a consequence, the pitching frequency is well apparent in the velocity spectra, as a sub-harmonic of the pitching frequency (see Figure 9).

Figure 9: Pitch and velocity spectra of the 1DOF LCO motion.

In Figure 10, turbulence intensity is seen to increase. Qualitatively, this increase in turbulence intensity can be seen in the time history plots. The fluctuations increase as the wake becomes more energetic with increasing Reynolds number. The efficiency is defined as the ratio of the extracted power $\bar{P}$over the power in the flow P_a.

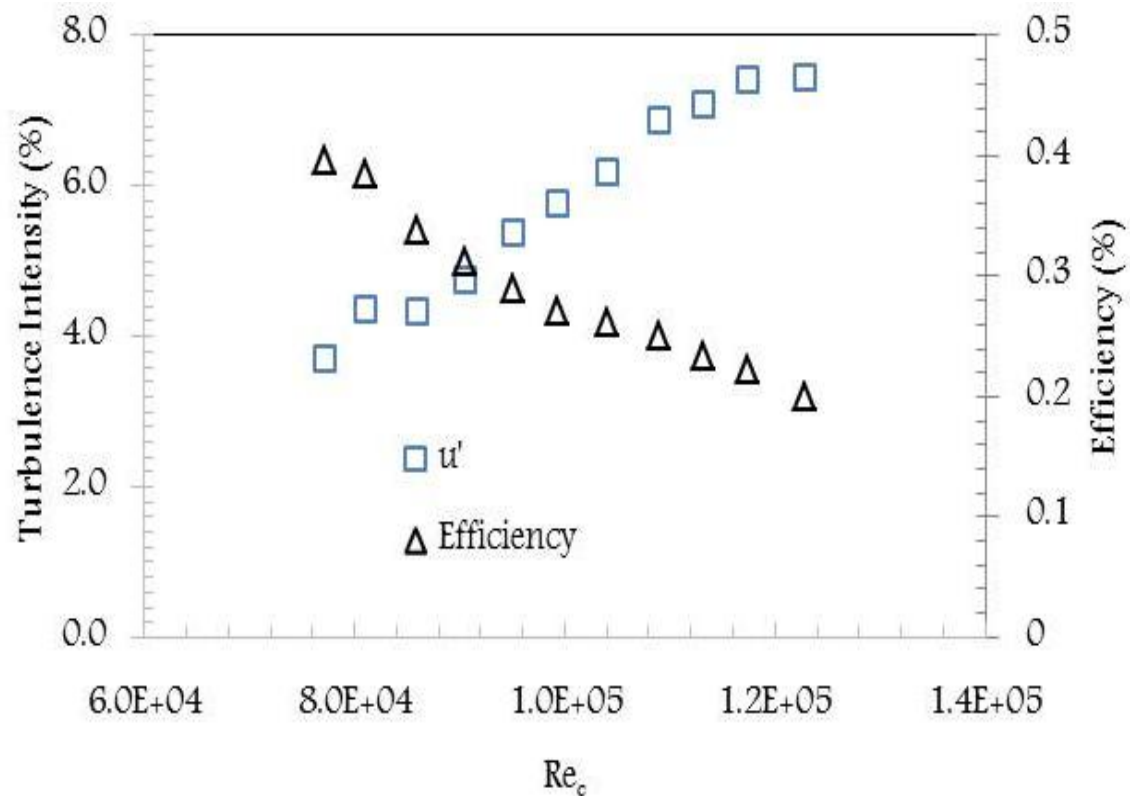$$\bar{P} = \frac{1}{T}\int_0^T [M_{EA}\,\theta]\,dt = \frac{D_\theta \overline{\theta^2}\,\omega^2}{2}$$

and

$P_a = \frac{1}{2}\rho.A.U_\infty^3$ A is the projected area.

$$\eta = \frac{\bar{P}}{P_a}$$

The efficiency η is also shown in Figure 8.The efficiency decreasesas more energy is shed into the wake with increasing Reynolds number. The results for the pitch amplitude, frequency, as well as aerodynamic efficiency were found to match well with previous results for the same set-up and conditions.

Figure 10: Turbulence intensity and efficiency during the 1DOF LCO motion.

Conclusion

Self-sustained oscillations were observed for a range of Reynolds numbers of $7.5 \times 10^4 \leq Re_c \leq 1.3 \times 10^5$. The amplitude of oscillations of the airfoil was determined as a function of air speed. It ranged from 32° to 47° for the pitch and from 1.5 cm to 3 cm for the heave. The frequency of both the pitch and heave increased almost linearly with air speed from 2.5Hz to 3.2Hz. The signals and the power spectra of *u* velocityin thewake for both 1DOF and 2DOF showed a clear signature of the oscillatory motion on the wake velocity. Turbulent spots pass at the measuring position at time intervals equivalent to half of the oscillation period. It results in the appearance of a dominant peak at twice the frequency of oscillation. The analysis of the turbulent spots shows that no Kármán vortices are present in the wake and that the scale distribution in these spots follows very well an inertial subrange behavior with a -5/3 power law. More experiments will allow a better understanding of the development of the wake downstream. Spectra will be extended to higher frequencies to capture the extent of the inertial sub-range. The lateral component of the velocity will provide extra information on the orientation of the flow passed the oscillating airfoil. Results of these investigations will be presented in the final version of this paper and during the conference presentation.

References

[1] Lee, T. &Gerontakos, P. "Investigation of flow over an oscillating airfoil", *Journal of Fluid Mechanics*, Vol. 512, pp. 313-341, 2004.

[2]Poels, A , Rudmin D, Benaissa, A, Poirel, D "Localization of Flow separation and Transition Over a Pitching NACA0012 Airfoil at Transitional Reynolds Numbers Using Hot-Films", *Journal of Fluids Engineering*, Vol. 137, 2015.

[3]Rudmin, D., Benaissa, A., and Poirel, D., "Detection of Laminar Flow Separation and Transition on a NACA-0012 Airfoil Using Surface Hot-Films", *Journal of Fluids Engineering*, Vol. 135, No. 10, 2013.

[4] Benaissa, A. & Poirel, D. "Study of Wake Flow Structure of a Self-Sustained Oscillating Airfoil", *ICAMEM*, Tunisia, 2007.

[5]Yuan, W, Poirel, D and Wang,B. "Simulations of Pitch–Heave Limit-Cycle Oscillations at a Transitional Reynolds Number"AIAA Journal Vol. 51, No. 7, July 2013.

[6] Onoue, K. & Breuer, K. "Vortex formation and shedding from a cyber-physical plate", *Journal of Fluid Mechanics*, Vol. 793, pp. 229-247, 2016.

[7] Huang, R.F.; Lee, H.W. "Frequency selection of wake flow behind a NACA0012 wing", *Journal of Marine Science and Technology,* vol. 6, no. 1, pp. 29-37, 1998.